# Resolving the Non-Productive Periods of Solar Chimney by Integrating with Waste-to-Energy Plant

Ali Habibollahzade, Ehsan Houshfar, Amir Mohammad Behzadi, Ehsan Gholamian and Mehdi Ashjaee



May 24, 2018

# RESOLVING THE NON-PRODUCTIVE PERIODS OF SOLAR CHIMNEY BY INTEGRATING WITH WASTE-TO-ENERGY PLANT

*Ali Habibollahzade*, Ehsan Houshfar, Amirmohammad Behzadi, Ehsan Gholamian, Mehdi Ashjaee*
*School of Mechanical Engineering, College of Engineering, University of Tehran, P.O. Box 11155-4563, Tehran, Iran*
*Corresponding author e-mail: *A.Habibollahzade@ut.ac.ir*

## ABSTRACT
Total global renewable energy capacity has been increasing worldwide, i.e. doubled from 2007 to 2016. The main disadvantage of most renewable energy based plants is the lack of reliability for constant electricity production. Solar chimney is a renewable based plant with a power production of near zero during the night times. In this study, we have proposed a renewable integrated cycle by combining two plants and thereafter produce a reliable amount of electricity all the time. The proposed combination is achieved by injecting outlet air from the condensers of Tehran's waste to energy plant into the bottom of the chimney tower, just below the turbine. Tehran's average climate data for 12 months of the year is initially obtained and the Manzanares prototype is used for the solar chimney power plant model. The solar chimney power plant is simulated with 3D CFD simulation. The final power output of the solar chimney power plant reaches 20–70 kW and increased 20%–1200%, compared to the case without injection. This means power output of solar chimney power plant is at least 20 kW in the hottest night of the year with 5% relative humidity. We have concluded that by combining these renewable based plants, one of the most important solar chimney disadvantages could be removed.
**Keywords:** Solar chimney power plant, Waste to energy, CFD, Renewable energy, Exergy

## 1. INTRODUCTION
Solar chimney power plants (SCPP) are among the technologies with high potential all over the world. SCPP consist of three main parts: first, solar collector to absorb solar heat, second, turbine that can be installed inside the chimney tower or within the collector area, and third, tower which is installed at the center of the collector (Schlaich et al., 2005). Solar radiation heats up the air under the collector and produces electricity by rotating the turbine blades. Unlike solar cells, SCPP can work day and night, since the pressure difference always exists between the inlet and the outlet of SCPP (Schlaich et al., 2005). For increasing power in nighttime, water bags can be placed under the collector to store heat in day and transfer to the surrounding air during nighttime, although electricity production would significantly be lower at such times (Schlaich et al., 2005). Few researchers further tried to resolve the instability power production of the SCPP using additional thermal storage, e.g., placing water bags on the soil (Zhou et al., 2010), using soil heat storage (Guo et al., 2016), and implementing solar ponds (Leffler et al., 2012). Using low temperature of geothermal brine as an external heat source was also investigated (Cao et al., 2014). Albeit these research works seem interesting, they can just prolong the power production time or produce little power in nighttime.

The purpose of this study is increasing SCPP power especially in nighttime and cold months of the year, since in such times the solar radiation is considerably lower. Hence, an integrated renewable system by combining Tehran's waste-to-energy (WtE) plant and an SCPP prototype is proposed. This is the first study to undertake a longitudinal analysis of the WtE-SCPP integrated systems, from a thermodynamic and fluid flow point of view. The air from condensers of Tehran's WTE is reused to increase SCPP power.

## 2. METHODOLOGY
Manzanares SCPP is integrated to the Tehran's WtE plant. The integration is performed by injecting the outlet condensers warm cooling air (the plant has two identical lines and two condensers) of the WtE plant into the SCPP just below the turbine. The injection is conducted using two pipes as shown in Fig. 1. At different months of the year, warm air has different temperature after passing the condenser. Therefore, simulation of the proposed cycle is done for 12 months of the year at the Tehran's WtE plant location.

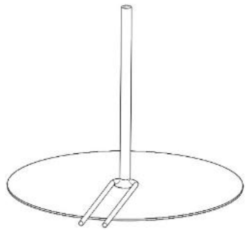

Fig. 1. A schematic of the injection method

The 3D simulation is conducted by ANSYS Fluent for SCPP. Following equations are used for simulation. The power output of the SCPP can be calculated as (Habibollahzade et al., 2018):

$$\dot{W}_{SCPP} = \frac{1}{3}\eta_T \eta_f \int V_T{}^3 \rho_T \, dA_t \tag{1}$$

Ambient air humidity should be considered for more realistic modeling. Relative humidity is calculated as follows:

$$\phi = \frac{P_v}{P_{sat\,@T_0}} \tag{2}$$

Additionally, the canopy convection heat loss coefficient is defined as (McAdams, 1954):

$$h = 5.67 + 3.86 \times V_{wind} \tag{3}$$

## 3. RESULTS AND DISCUSSIONS

### 3.1 COMPUTATIONAL FLUID DYNAMICS SIMULATION

ANSYS Fluent is used for simulating the SCPP. The turbulence model *k–ε RNG* is selected with full buoyancy effect for viscous modeling. Soave-Redlich-Kwong equation is used for calculation of the real gas density. The coupled scheme is used for the pressure-velocity coupling. Second order upwind method is applied to density, momentum, and energy to achieve a better solution accuracy.

#### 3.1.1 GRID INDEPENDANCY

The SCPP domain is meshed with hybrid type cells. Hexahedral structured mesh is generated for the collector and tetrahedral unstructured mesh for the chimney tower. To ensure the outcomes, grid independency is initially investigated. By increasing number of elements from 2,189,764 to 4,452,308, upwind velocity is changed only 0.05%. Therefore, 2,189,764 elements are chosen for further simulation of cases without injection.

Also, grid independency is tested for cases with air injection. Results show that by increasing number of elements from 3,390,058 to 6,256,211, solution is changed maximum 0.07%. Hence, 3,390,058 elements is chosen for the simulation.

#### 3.1.2 SCPP MODEL VALIDATION

To validate the SCPP model of this study, data reported by Weinrebe and Schiel (Weinrebe and Schiel, 2001) on 8th June 1987 is used. Main boundary conditions and geometry specifications for modeling the SCPP are tabulated in Table 1. Comparison of present numerical results and experimental results of Manzanares prototype are shown in Table 1, where a maximum error of 6.5% is reported.

Table 1. Comparison between present results with available experimental and simulation results

| Parameter | Measured (Weinrebe and Schiel, 2001) | Simulated by Weinrebe and Schiel. (Weinrebe and Schiel, 2001) | Present simulation |
|---|---|---|---|
| Temperature at collector exit (°C) | 38 | 41 | 40.45 |
| Upwind velocity (m/s) | 8.1 | 8.0 | 8.03 |
| Power output (kW) | 48.4 | 48.5 | 48.10 |

### 3.2 AIR INJECTION RESULTS

After air injection, the power output of the SCPP is changed notably. Average power increase in different months of the year is investigated and illustrated in Fig.2. As Fig. 2. shows, power increase is higher in cold months of the year. Considering averaged monthly data, 65–94% power increase is achieved with injection. Power output of the SCPP is between 40 kW and 50 kW averagely in different months. Additionally, temperature, pressure contours at the walls (canopy glass, pipes and tower walls) and cut-plane velocity contour of SCPP is shown in Fig. 3.

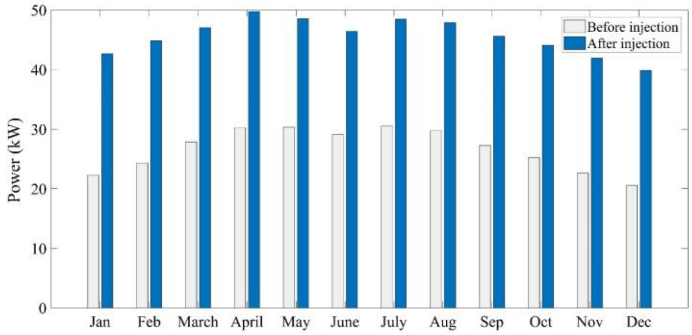

Fig.2. the power output of the SCPP turbine before and after injection in different months

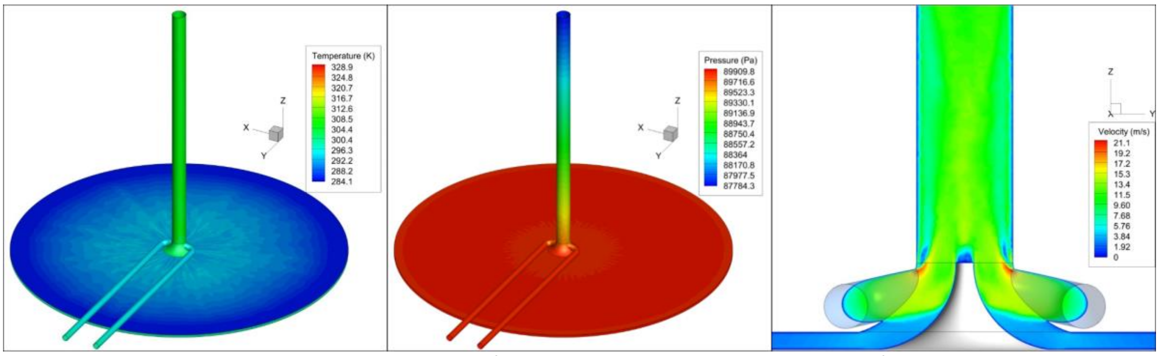

Fig. 3. Temperature, pressure contours at the walls (canopy glass, pipes and tower walls) and cut-plane velocity contour of SCPP

The base case of the proposed integrated cycle is modeled at $T_0$=25 °C, $P_0$=90 kPa, $V_{wind}$=2.5 m/s, $\phi$=30%, $\dot{m}_{condensers}$=420 kg/s.

Since the condensers mass flow rate vary by varying the municipal solid waste mass flow rate and humidity, so the condensers mass flow rate is not constant. Effect of condensers mass flow rate on SCPP power output is investigated in Fig. 4(a). As the figure shows, by increasing the condensers mass flow rate, power of the SCPP increases significantly.

Another important parameter that has an essential role on the power output of the SCPP is the wind speed. According to Eq. (3), by increasing the wind speed, convective heat transfer increases and this means higher heat loss from the walls. In this study, in addition to the heat loss from the collector roof, the heat loss from the pipe walls is also considered. According to Fig. 4(b), by increasing the wind speed above the collector, power generation of the SCPP is decreased but as wind speed increases from 5 m/s to higher values, amount of power reduction is not noticeable. Moreover, there is almost no power reduction in the wind speeds of 12.5 m/s and higher. In addition, the power production during the nighttime is almost independent of the wind speed. As the solar radiation increases, the wind speed becomes more effective. It can thus be suggested that the power output of the SCPP could be 25% higher when the solar radiation is high and the wind speed is close to zero.

Relative ambient air humidity could increase power generation of the SCPP up to 25% in high relative humidity as shown in Fig. 4(c). The increase in power is almost linearly correlated with the solar radiation at various relative humidity.

Ambient air temperature is also effective on the SCPP power generation. Increasing air temperature will lower the power production because of the lower air density. Fig. 4(d) shows that power production is higher in higher ambient temperatures during the night (zero solar radiation) due to the fixed relative humidity ($\phi$=30%). As discussed, the relative humidity can considerably affect the results. According to Eq. (2), since the specific humidity is directly related to the ambient temperature, higher ambient temperature means higher steam mass and therefore higher speed and higher power production. This is true if the mass flowrate inside the solar chimney is low enough, e.g., during the nighttime. As solar radiation increases, the mass flowrate inside the chimney increases too, and the power production will be higher in lower ambient temperatures. At 200 W/m$^2$ solar radiation, power production is independent of the ambient temperature because of the fixed relative humidity. As shown in Fig. 4(d), 63.8 kW power production requires 900 W/m$^2$ of solar radiation in the ambient temperature of −5 °C and 1040 W/m² in 35 °C ambient temperature with similar effective parameters; although such a high solar radiation is impractical in cold conditions.

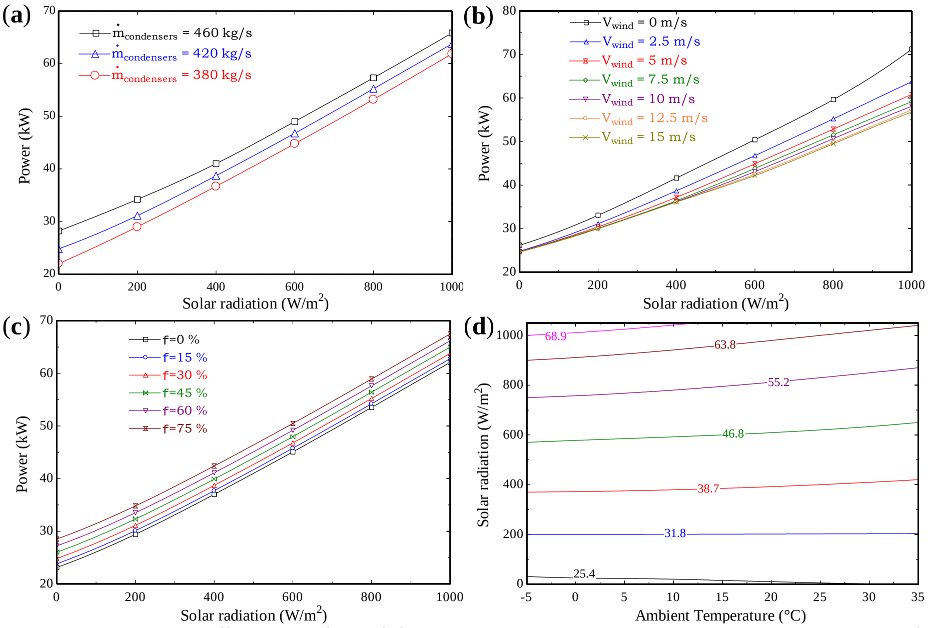


Fig. 4. a) power output and exergy efficiency of the SCPP versus solar radiation in various $\dot{m}_{condensers}$ b) power output of the SCPP as a function of solar radiation at different wind speeds c) power output of the SCPP as a function of solar radiation at various ambient air relative humidity d) effect of solar radiation and ambient temperature on the power output of the SCPP

## 4. CONCLUSION

In this study, the warm air stream from the condenser of the WTE plant is reused to increase power output of the SCPP especially in cold months and nighttime. Injection of the air is examined with different geometric conditions. A 3D CFD simulation of the SCPP is performed for different monthly climate data of Tehran. Furthermore, a comprehensive thermodynamic analysis is done for the WTE plant. The results of the proposed integrated renewable plants suggest minimum 20% power increase at high radiation days and maximum 1200% during nights for the base case and even higher power increase in other conditions. The increase rate of power in nights and cold months is much higher and minimum power generation is never less than 20 kW. Furthermore, a 20–1200% power increase of the SCPP for the base case after injection and 65–94% monthly average power increase is reached.

## REFERENCES

Cao, F., Li, H., Ma, Q., Zhao, L., 2014. Design and simulation of a geothermal-solar combined chimney power plant. Energy Convers. Manag. 84, 186–195. https://doi.org/10.1016/j.enconman.2014.04.015

Guo, P., Wang, Y., Li, J., Wang, Y., 2016. Thermodynamic analysis of a solar chimney power plant system with soil heat storage. Appl. Therm. Eng. 100, 1076–1084. https://doi.org/10.1016/j.applthermaleng.2016.03.008

Habibollahzade, A., Houshfar, E., Ashjaee, M., Behzadi, A., Gholamian, E., Mehdizadeh, H., 2018. Enhanced power generation through integrated renewable energy plants: Solar chimney and waste-to-energy. Energy Convers. Manag. 166, 48–63. https://doi.org/10.1016/j.enconman.2018.04.010

Leffler, R.A., Bradshaw, C.R., Groll, E.A., Garimella, S. V., 2012. Alternative heat rejection methods for power plants. Appl. Energy 92, 17–25. https://doi.org/10.1016/j.apenergy.2011.10.023

McAdams, W.H., 1954. Heat Transmission, 3rd ed. ed. McGraw-Hill, New York.

Schlaich, J., Bergermann, R., Schiel, W., Weinrebe, G., 2005. Design of Commercial Solar Updraft Tower Systems—Utilization of Solar Induced Convective Flows for Power Generation. J. Sol. Energy Eng. 127, 117. https://doi.org/10.1115/1.1823493

Weinrebe, G., Schiel, W., 2001. Up-Draught Solar Chimney and Down-Draught Energy Tower - A Comparison. ISES 2001 Sol. World Congr. 14.

Zhou, X., Wang, F., Ochieng, R.M., 2010. A review of solar chimney power technology. Renew. Sustain. Energy Rev. 14, 2315–2338. https://doi.org/10.1016/j.rser.2010.04.018